



UNIVERSITY OF AMSTERDAM

FINAL YEAR THESIS

**Study of oscillons in $1+1D$ with a
gentle introduction to multi-
component oscillon models**

Athul Muralidhar

supervised by
Dr. Marieke POSTMA
Dr. Evangelos SFAKIANAKIS

September 28, 2018

Dedicated to Viji and Murali, without whome any of this wouldn't have happened!

Contents

1	Introduction	3
2	Non-Linearity, Integrability and Soliton solutions	5
2.1	The sine-Gordon soliton	7
2.2	The Q-ball	10
3	Oscillons	11
3.1	Oscillon model in 1+1D	13
4	Computational details	17
4.1	The Runge-Kutta Method	17
4.2	The Shooting method	18
4.2.1	The Secant method[5]	19
4.3	Finite differencing	19
5	Oscillon Energy and time evolution	20
6	Multicomponent oscillon models:	23
A	Quantum Mechanical operators[?, 41]:	25
B	Euler-Lagrange equation[42]:	26
C	Cosmic Inflation:	28
D	Tests on the Runge-Kutta method:	29
D.1	The source-code used:	30
E	Testing the shooting method:	33
E.1	The source-code used:	34
F	The source code used for this work:	38
F.1	Oscillon profile:	38
F.2	Oscillon evolution:	41
F.2.1	Python version	41
F.2.2	Go version:	43

1 Introduction

Waves and the study thereof has always been an integral part of the realm of Physics. They are found in a myriad of natural phenomena and as such form an integral part in our understanding of the world around us. Examples include mechanical waves like water waves, sound waves and seismic waves which use vibrations of matter in order to propagate, while other examples like light waves and de Broglie waves use oscillations of electric and magnetic fields for propagation. With the advent of Quantum mechanics and other advanced theories, the study of waves and wave theory has yet again captured the centre stage in most areas of Physics.

Among the various interesting phenomena that are associated with waves and wave propagation, the majority of the current work deals with the unusual phenomenon called the *Wave of Translation* or a *Solitary wave*. The first reported description of this phenomenon comes as early as 1834, when a Scottish Civil Engineer, John Scott Russell[7, 8] while conducting experiments to determine the most efficient design for canal boats, discovered that after observing the motion of a boat being rapidly drawn along a narrow channel by a pair of horses, after being stopped, created a mass of water in the channel which accumulated around the prow of the vessel. The violent agitation, then suddenly leaving the boat behind, rolled forward with great velocity, assuming the form of a large solitary elevation, a rounded, smooth and well-defined heap of water, which continued its course along the channel apparently without change of form or diminution of speed. After some intensive practical and theoretical investigations of these waves, he found that this kind of waves were stable, and can travel over very large distances without flattening, steepening or toppling over. Their speed depended on the size of the waves, and their width on the depth of water. Unlike normal waves they never merged with one other. It is interesting to note that these observations seemed to contradict the working water-wave theories of those times, which were developed by stalwarts like Newton and Bernoulli.

The first mathematical understanding of the Solitary waves were pioneered by Joseph Valentin Boussinesq and Lord Rayleigh[6] during the 1870s and later expounded by Gustav de Vries¹ and Frederik Korteweg². They devised the Korteweg–de Vries equations[9] (KdV equations), which follows from a mathematical model with exactly solvable solutions involving non linear partial differentials. The model had solitary wave like properties thereby adding further credibility to the already unusual phenomenon. The study of the Solitary waves had become a serious research topic by the early 1960s. By 1965, Norman Zbarsky of Bell Labs and Martin Kruskal[10] of Princeton University demonstrated the solitary wave behaviour in media in a computational investigation using a finite difference approach and after a couple of years, Gardner, Greene,

¹Was an Alumni of the University of Amsterdam and had studied with Johannes van der Waals

²Was the recipient of the first ever PhD in mathematics awarded by the University of Amsterdam

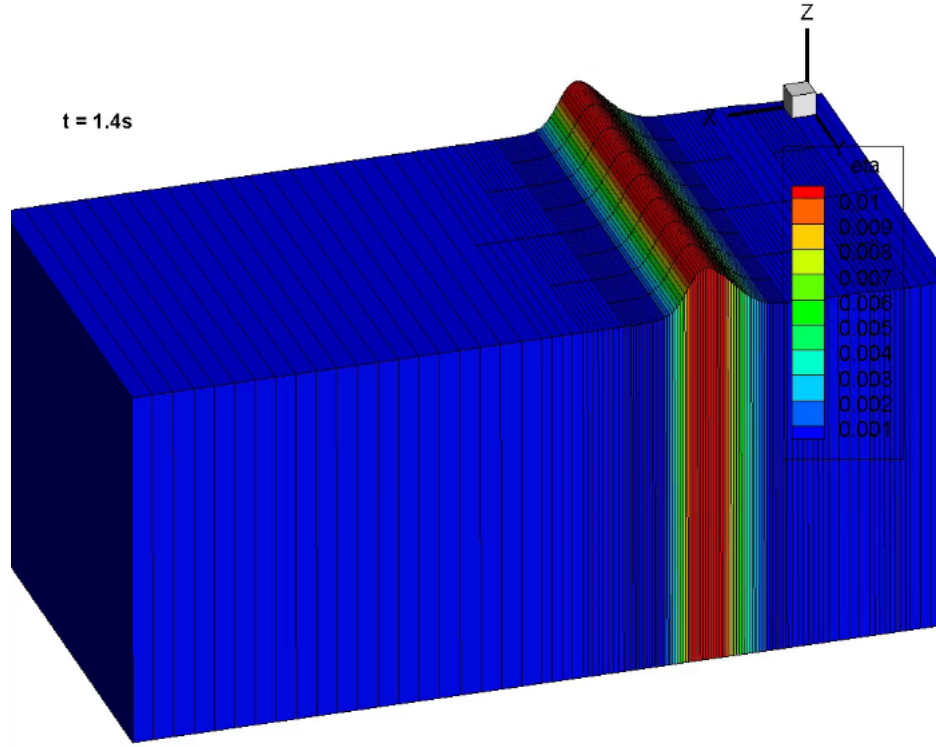


Figure 1: A snapshot of a solitary wave in water[43]

Kruskal and Mira discovered an inverse scattering transform enabling analytical solution of the KdV equation.

By this time, the Solitary waves or *Solitons* were fairly established in various fields of Physics, both experimentally and theoretically. The description now ascribes to a self-reinforcing solitary wave packet that maintains its shape during its propagation at a constant velocity due to a cancellation of non-linear and dispersive effects in the medium of propagations. This is technically a slightly different conception, different from the Solitary wave description mentioned in the late 1800s as the Solitary waves after interaction with each other change slightly in amplitude leaving behind an oscillatory residue which by definition is not seen in a Soliton[11].

2 Non-Linearity, Integrability and Soliton solutions

Differential equations are equations which relate certain functions with their derivatives. These equations have wide spread applications ranging from biological sciences to modern economics. Having been invented by the fore-runners of scientific thought³, they have found various applications in the fields of Mathematics and Physics. Vibrating strings and oscillations were naturally expressed in these forms of equations and their study invariably dealt with the solving of these equations and studying the properties of the solutions. Unlike algebraic equations, these equations can be notoriously difficult to solve, hence the existence, methods and study of solutions are an active field of research in Mathematics and Physics.

A function $f(x)$ is said to be *linear* when it satisfies both[12]:

$$\begin{aligned}f(x + y) &= f(x) + f(y) \\f(\alpha x) &= \alpha f(x)\end{aligned}$$

The former is the additivity principle, while the later is the homogeneity principle which together imply that the function f follows the *superposition* principle. In terms of differential equations, the linearity principle translates to the reducibility of the differential equations. A linear *Ordinary Differential Equation*(ODE)⁴ or a linear *Partial Differential Equation* (PDE)⁵ can be written in simpler forms and their solutions added to get to the original solution, thus making them slightly easier to solve for[13]. On the other hand, non-linear(NL) ODEs or PDEs do not follow the superposition principle and hence the solvability of the equations is itself then a question to be answered.

In spite of the fact that the NL- ODEs or PDEs can be troublesome to solve, they arise quite naturally in physical phenomena making them indispensable ingredients for the study of those phenomena. One glaring example is the equation of motion for a classical simple pendulum under the influence of gravity. This equation can be arrived at by assuming that the gravity acts downwards, pulling the string of the pendulum and the angle subscribed by the pendulum during its periodic swinging using the Lagrangian formulation of Newton's equations of motion.

There may arise some ambiguity about the term *linearity* as physicists and mathematicians use the term in varying levels of meaning. Our discussions above have strictly a mathematical character, particularly the simple pendulum for a mathematician is a *non-linear* problem as the partial differential equations that describe it are strictly non-linear[13], while for a physicist, the simple pendulum is a *linear* system as one can add infinitely many simple pendulums together

³Newton, Leibniz, d'Alembert, Euler, Bernoulli, Lagrange etc.

⁴differential equations involving only one variable

⁵differential equations involving multiple variables

and the equations do not intermix between the different individual pendulums and hence each can be solved independently of the other. Nevertheless, they agree on the meaning of linearity when talking about wave mechanics[14]. We will encounter non-linear equations in the next sub section.

When a certain number of ODEs or PDEs, irrespective of their linearity act together to describe a particular system, then they form a system of differential equations that describe the system. These sets of differential equations have to be simultaneously solved to arrive at the solutions. An *integrable system* is then defined as a system in which the differential equations of the respective system, determined by their appropriate initial conditions can be integrated or solved completely[30]. These integrable systems are of particular interest physically as they give raise to many conserved quantities⁶ of those particular systems. One of the simplest classical non-linear integrable system is the *Simple Harmonic oscillator*⁷ (SHO) which follows the Hooke's law and with the equation of motion described as:

$$\frac{d^2x}{dt^2} + \frac{kx}{m} = 0$$

here, the spring's motion is assumed to be in the x direction, the spring constant is k with a spring mass m . Moving to the quantum mechanical analogue of this system, from classical wave theory[15] we have:

$$\frac{\partial^2}{\partial x^2}\psi(x, t) - \frac{1}{c^2} \frac{\partial^2}{\partial t^2}\psi(x, t) = 0$$

where ψ is the wave function defined at every point in space and time and c is the speed of the wave. In the non-relativistic limit i.e in regimes where the particle velocity is much smaller than the speed of light, we define the energy of a free particle and its momentum as:

$$E = \frac{p^2}{2m}$$

and using the Einstein - de Broglie equations[16], we get:

$$\hbar\omega = \frac{\hbar^2 k^2}{2m}$$

Identifying that the energy and momentum become operators that operate on a wave function in quantum mechanics(Q), we get the time dependent *Schrödinger equation*[20] given by:

$$i\hbar \frac{\partial}{\partial t}\psi(x, t) = -\frac{\hbar^2}{2m} \frac{\partial^2}{\partial x^2}\psi(x, t)$$

we are still assuming that the particle lives in one space dimension (x) and oscillates in time. For a particle that is bound to a potential V , the above

⁶Not always the case as we shall see later

⁷one of my personal favourite topics of study in Physics

equation is slightly modified, but a particular choice of the potential $V = 1/2kx^2$ leads to the Q equivalent of the simple harmonic oscillator[21]:

$$i\hbar \frac{\partial}{\partial t} \psi(x, t) = -\frac{\hbar^2}{2m} \frac{\partial^2}{\partial x^2} \psi(x, t) + \frac{1}{2} kx^2 \psi(x, t)$$

Although the equations for both the oscillators look similar, certain subtleties do exist. The total energy of the classical SHO can be any positive number, while in the Q version, only discrete states are allowed to exist. In Q, we are concerned with the *probabilities*[17] of finding a particle in a particular energy state, and sometimes we have non-zero probabilities of finding the particle completely outside of our potential barrier⁸[18]. Moreover the lowest energy state in a QM-SHO is non-zero, and it is referred to as the *zero point energy*[19] of the system. In spite of the inherent fuzziness in the theory, Q has time and again been proved right in various experiments and observations[22, 23, 24].

2.1 The sine-Gordon soliton

Continuing from our previous discussions of the Q simple harmonic oscillator, our aim is to extend this simple system into understanding the quantum realm of our universe. Imagine a QM-SHO defined at every point in space-time and each connected to the other with some form of a massless elastic thread such that the vibrations of one SHO is not independent of the other surrounding SHOs. We have now invented what mathematicians and physicists call a *field*. Technically a field is defined as a physical quantity that has a specific value at every spacetime point[25, 26]. With our above analogy of the QM-SHO, a field then represents certain energy states of the SHOs that is defined at every point in spacetime. The scenario is fairly complex than the simple SHOs as they are now coupled to their neighbours and evidently necessitates a change from the usual Q approach of studying the system[26].

The Schrödinger equation works for both electrons and photons in non-relativistic regimes but it breaks down when we increase the velocities of these particles to approach the speed of light⁹. It also becomes inefficient in our study of the infinitude of QM-SHOs, as spacetime extends infinitely having infinitely many spacetime points due to it being *continuous*. The indistinguishability of the Q particles also adds to the problem as we also run into the risk of double counting the particles. The breakthrough came when physicists like Paul Dirac constructed equations that kept track of the *number* of particles in a given energy state rather than individually describing each particle and its respective state. This approach came with added advantages of being able to accommodate the *creation* and *annihilation* of particles¹⁰[26]. As the mathematics of Q and going further, *Quantum Field Theory*(QFT) can get tedious, we make two

⁸this phenomenon is called tunnelling

⁹the equation does not account for relativistic effects(time dialation, length contraction etc.)

¹⁰one of the things that Mr.Schrödinger was completely silent about

simplifying assumptions that pertain to the system studied by this work. We are only interested in fields that do not obey the *Pauli exclusion* principle or otherwise known as *Scalar* fields, the quantization of which are photon like particles called *bosons*¹¹ and that our Universe is flat, i.e. the spacetime co-ordinates in our equations are not *curved* and live in only one spatial dimension and one temporal dimension.

With the above pre-requisites we are ready to begin our investigations into the theory of quantum fields, QFT. Extending the previous discussions of QM-SHOs, let us now construct a field theory version of the same. From Lagrangian Mechanics, we redefine the classical Lagrangian into *Lagrangian density* \mathcal{L} , as we are now involved in computing the Lagrangian at the infinite points of space-time, and hence the usual description loses its meaning. We then define the Lagrangian density of the scalar quantum field $\phi(x, t)$, defined at every space-time point as[26]:

$$\mathcal{L}_{\text{KG}} = \frac{1}{2} \left((\partial_t \phi)^2 - (\partial_x \phi)^2 \right) - \frac{1}{2} m^2 \phi^2$$

here ∂_t and ∂_x describe partial differentiation with respect to time and space respectively and m is the mass of the scalar field. Solving the *Euler-Lagrange* equations using the given Lagrangian density we obtain the *Klein-Gordon equation*¹².

$$\frac{\partial^2 \phi(x, t)}{\partial t^2} - \frac{\partial^2 \phi(x, t)}{\partial x^2} + m^2 \phi(x, t) = 0 \quad (1)$$

Note that the \hbar 's and c 's have disappeared from the equation as we are now working in normal units where $\hbar = c = 1$. To the Klein-Gordon Lagrangian, adding higher order terms in powers of ϕ^2 , we get the *sine-Gordon*¹³ [27] Lagrangian density:

$$\begin{aligned} \mathcal{L}_{\text{SG}} &= \mathcal{L}_{\text{KG}} + m^2 \left(\frac{\phi^4}{4!} - \frac{\phi^6}{6!} + \frac{\phi^8}{8!} + \dots \right) \\ \mathcal{L}_{\text{SG}} &= \mathcal{L}_{\text{KG}} + m^2 \sum_{n=2}^{\infty} \frac{(-\phi^2)^n}{(2n)!} \end{aligned}$$

The infinite series is then recognized as the Taylor expansion of the cos function, then the equation becomes:

$$\mathcal{L}_{\text{SG}} = \frac{1}{2} \left((\partial_t \phi)^2 - (\partial_x \phi)^2 \right) - 1 + \cos(\phi) \quad (2)$$

The corresponding Euler-Lagrange equations of motion for the sine-Gordon Lagrangian density is given by[27]:

¹¹the fields that obey the Pauli exclusion principle, called the vector fields, quantize into particles like electrons, quarks etc.

¹²for the more inquisitive the metric signature is $(+, -)$

¹³this is essentially a pun on the Klein-Gordon equation!

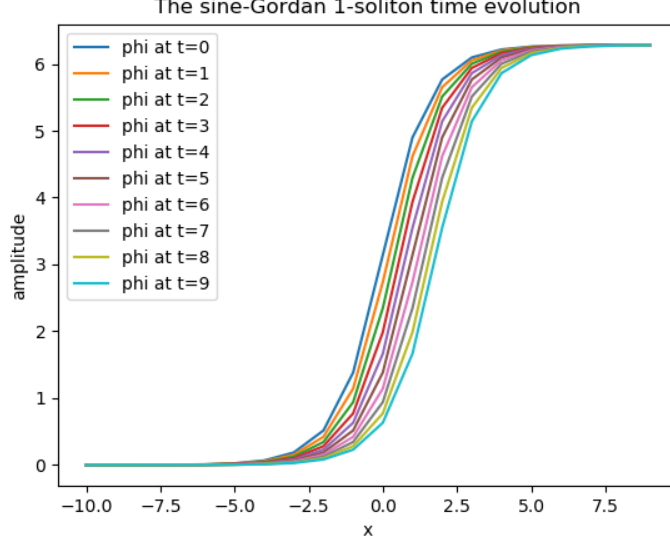


Figure 2: The sine-Gordan 1-soliton kink solution plotted at different times. We have set $m = +1$, $x_0 = 0$ and $c = 0.2$

$$\partial_{tt}\phi - \partial_{xx}\phi + m^2 \sin(\phi) = 0 \quad (3)$$

The sine-Gordon model is of interest to us as the equations above have soliton solutions. Solving the above equation, we arrive at the one-soliton solution given by[28, 31, 32]:

$$\phi(x, t) = 4 \arctan \left(\exp \left(\pm m \frac{x - x_0 - ct}{\sqrt{1 - c^2}} \right) \right)$$

the above equation represents a localized solitary wave, travelling at any velocity $|c| < 1$. The \pm signs correspond to localized solutions which are called *kink* and *antikink*, respectively. In fact, the equation(3) allows multiple solutions of the form[31]:

$$\phi(x, t) = 4 \arctan \left(m \left(\frac{F(x)}{G(x)} \right) \right)$$

where F and G are arbitrary functions. Another interesting solution for the sine-Gordon equation is the *breather* solution.

Breathers are non-linear anomalies found in wave theory characterised by being localized in space and oscillate (breathe) in time or vice versa. They are

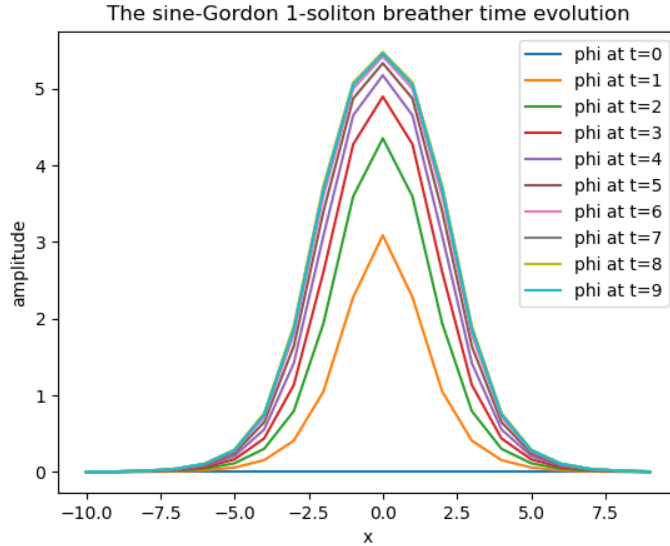


Figure 3: The sine-Gordon 1-soliton breather solution plotted versus time. As before, we have set $m = 1$ and $\omega = 0.2$

also called *oscillons*¹⁴. The breather mode for the sine-Gordon equation is given by[?, 33]:

$$\phi_B(x, t) = 4 \arctan \left(m \frac{\sqrt{1 - \omega^2} \sin(\omega t)}{\omega \cosh(\sqrt{1 - \omega^2} x)} \right)$$

which is periodic for frequencies $\omega < 1$ and decays exponentially when moving away from $x = 0$.

2.2 The Q-ball

One of the prime requirements of any valid Physics theory is that the equations so derived must stay the same regardless of who measures the predictions of such a theory anywhere in the Universe. In other words, if the equations are subject to rotations, translations or other *transformations*, they must remain *invariant*[34], or unchanged under that transformation. For example, if we were to predict the trajectory of the earth revolving around the Sun, according to Newton's laws of motion, another observer far away from earth should end up with a trajectory similar to ours meaning that Newton's laws of motion are then invariant. There is a more subtler notion that the invariance points to, the *symmetry* of Newton's laws of motion. The notion of symmetry is very much

¹⁴more in the following sections

prevalent in natural phenomena. In essence “it is only slightly overstating the case to say that physics is the study of symmetry” to quote the Nobel Laureate P.W. Anderson[35]. Mathematically speaking, the cumbersome equations emergent from natural phenomena can be easily simplified and generalized by understanding the underlying symmetry of such phenomena.

Emmy Noether, a pioneering mathematician while working on the calculus of variations discovered a fundamental theorem in her namesake which gives the connection between symmetry and conserved quantities. Unlike quantities that can be conserved in a physical sense, like energy and charge, Noether described an abstraction of these conversations and showed that every differentiable symmetry of the *action*¹⁵ of a physical system has a corresponding conservation law leading to a conserved quantity, the *Noether charge* associated with the system[36, 37]. This was indeed a phenomenal breakthrough in the field of Physics and Mathematics, which spurred a new revolution in the respective fields.

The *Q-ball*, then is a non-linear soliton solution of a field configuration stabilized by the conserved Noether charge of the system. They are *non-topological*, meaning that they do not arise from defects in the spacetime describing the field[38]. Q-balls were introduced by Sidney Coleman[39], by describing a bosonic field configuration whose existence is guaranteed by the field equations if: 1) the potential grows slower than the quadratic mass term of the particle 2) the energy(mass) of a Q-ball is lower than the corresponding energy of a collection of the lightest possible scalar particle quanta 3) the energy of a single Q-ball is less than the total energy of the smaller Q-balls that it could fragment into and 4) the Q-ball not being strongly coupled with fermions. With the above preliminaries in place, we are ready to delve into the main focus of this work, the study of oscillons in a 1+1 dimensional spacetime[29].

3 Oscillons

Oscillons are long-lived field configurations that are localized in space and oscillate in time. They are objects that arise in scalar field theories, when a non-linearity in the field potential can balance or nullify the effects of the dispersion relations governing them. They are non-topological and not completely stable, but nevertheless can last for thousands of oscillations. Hence they can have significant cosmological consequences, if they are formed after inflation¹⁶. A number of physical phenomena from water waves travelling in narrow canals, to phase transitions in the early Universe exhibit the formation of localized, long-lived energy density configurations, even without gravitational interactions. Some of these configurations are surprisingly stable due to the conservation of topological or non topological charges, while some are unusually long lived due to a dynamical balance between the non-linearities and other dissipative forces.

¹⁵A quantity that is constructed based on the Lagrangian of a system

¹⁶cf. Appendix C

Well-studied examples include topological solitons in the 1+1-dimensional Sine-Gordon model and non topological solitons such as Q-balls. In case of the Sine-Gordon soliton, it is stationary in time, whereas the Q-balls are oscillatory in nature. Both have conserved charges, which make them stable, at least in cases where the coupling to gravity is minimal. Another interesting example of such localized configurations are called oscillons. Like the Sine-Gordon soliton, oscillons can exist in real scalar fields, and like the Q-balls they are oscillatory in nature but however, unlike both of the above examples they do not have any known conserved charges. In general they decay, but their lifetimes are significantly longer than any natural time scales indicated by their respective Lagrangians. Along with their longevity, another fascinating aspect of oscillons is that they emerge naturally from relatively arbitrary initial conditions. Relativistic, scalar field theories with non-linear potentials form simple yet interesting candidates for studying such phenomenon. While oscillons have been shown to exist in many models and their properties have been studied using various possible influence on the initial conditions, there is only a handful of scientific papers dealing with oscillons made up of two fields or more fields. This is an important oversight, since realistic high energy physics theories like string theory and supersymmetry are striking examples. These models are likely to include a variety of interacting scalar fields.

In the context of String theory, scalar fields generally describe the size and shape of extra dimensions involved. These string compactifications, called *moduli* fields provide ample seed structures for oscillon formation. With a high number ($\mathcal{O}(100)$) of such fields arising naturally from such theories, it is then imperative to study their cosmological importance. Oscillons may dominate the energy density of the Universe before they radiate and decay, delay thermalization to some extent and may even be sources of baryon asymmetry. A detailed study of the string compactifications in Type IIB string theory[44], concludes that these moduli fields may even be the only remnants of string theory surviving after cosmic inflation.

The origins of large scale structure that we see today in the Universe can be traced back to the density fluctuations in the primordial plasma[49]. After inflation, these fluctuations became the seed for all the galaxies, stars and other astronomical objects that we see today. The post inflationary inflaton field begins to oscillate around the minimum of its potential, decaying slowly into the Standard Model (SM) particles. This scenario can give rise to copious oscillon production in the early Universe as the inflaton potential, being minimally coupled to the SM particles can be self-resonant and produce quanta of the inflaton field more efficiently than the coupled particles[51]. Moreover if these oscillons have a lifetime comparable to the Hubble time during their formation, they can have significant cosmological implications[53] such as determining the phase transitions of the early Universe.

Although the inflaton field is insensitive to the actual shape of its potential, some theoretical and observational bounds can be made in light of oscillon

production[51]. With the CMB data collected from experiments like WMAP and Planck mission, the current upper bounds to the tensor to scalar ratio r , stands at < 0.09 , with a 2σ significance. Combining this with the scalar spectral index measurements, it seems likely that cubic and quartic potentials are highly disfavoured by the data[52]. The potential must also flatten out at larger values ($V(\phi) \gg m_{pl}^{17}$) to support inflation[53]. Hence, we are concerned in the present work with the inflaton potential around regions where $V(\phi) \ll m_{pl}$, such that the non-linear terms can be safely introduced as a Taylor truncated series of the original potential[53] with conditions matching the observations at high field values providing the setup for parametric resonance. The resonance then generates inhomogeneities that relax to form oscillons[51].

The oscillon potential must also be shallow than quadratic near the minimum such that the resulting scalar self interaction remains attractive[54]. This can then lead to oscillon production with large enough mass (energy) effectively localised in space[53]. The massive oscillons act as energy sinks of the expanding Universe and push it into the oscillon matter domination after which the Universe is reheated, entering the radiation domination era[54]. Due to the very nature of oscillons being energy sinks, they can be excellent sources for gravitational wave production[52] and primordial Black Hole formation[54].

We start by examining the models described by Amin et al[1] where they discuss flat-top oscillon solutions which are spatially localised and are long lived in time. They are also highly stable against long wavelength perturbations which makes them prime candidates for post inflation pre-reheating scenarios[53]. With the intuitive reasoning from Sfakianakis[?], we begin by understanding oscillons in 1+1D, i.e one spatial and one time dimension in a non expanding Universe.

3.1 Oscillon model in 1+1D

We define the standard Lagrangian density for a scalar field with a potential V , analogous to ref[?]

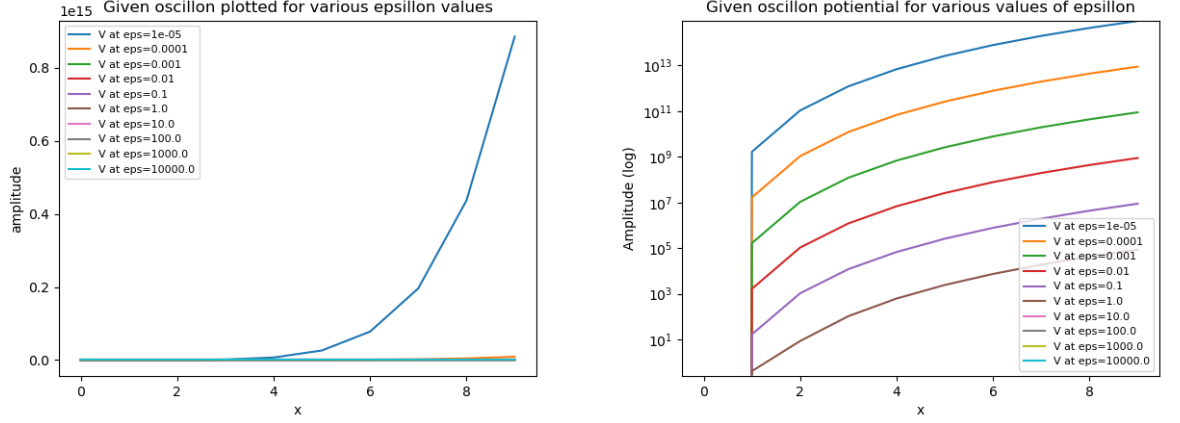
$$\mathcal{L} = \frac{1}{2} ((\partial_t \phi)^2 - (\partial_x \phi)^2) - V(\phi) \quad (4)$$

with

$$V = \frac{1}{2}\phi^2 - \frac{1}{4}\phi^4 + \frac{\Lambda}{6\epsilon^2}\phi^6$$

where the scalar field is represented by ϕ , limiting to the sixth power for the potential. In accordance with scalar field theory, the second power, the fourth power and the sixth power of the scalar field do indeed have their respective coefficients, but the coefficients for the later is the only one relevant for our discussions here. This is characterised by the setting of the coefficient for the second order (*mass*) and the coefficient for the fourth order (*Fermi*) are set to unity without the loss of generality. The sixth power is characterised by two

¹⁷ m_{pl} is the reduced Planck mass



(a) The given oscillon potential plotted for various values of ϵ , (b) The given oscillon potential plotted for various values of ϵ , range(1e-5,1e+5) using the log scale

non-zero parameters denoted by Λ and ϵ . The scenario is further simplified by considering a flat, non expanding universe ($H = 1$)¹⁸. The ϵ parameter is a small (constant) number which we will encounter later in our discussions and here it is an indicator that points to fact that the strength of the ϕ^6 term is a function dependant on the ratio between the Λ parameter and the ϵ parameter. The Λ parameter is proportional to the sixth order coupling strength of the scalar field, which is usually denoted by the letter g . The equation of motion (EOM) for the scalar field is given by:

$$\frac{d^2\phi}{dt^2} - \frac{d^2\phi}{dx^2} + \phi - \phi^3 + \frac{\Lambda}{\epsilon^2}\phi^5 = 0 \quad (5)$$

The oscillon profile can be extracted from the EOM with the change of variables from t to τ given by $\tau = \epsilon^2 t$ and from x to ρ given by $\rho = \epsilon x$. This is indeed the case as we have effectively introduced the ϵ parameter to the coordinate spacetime and we are now equipped to study the oscillon profile in this “diluted” spacetime. As the oscillons are oscillating only in time and are localized in space, we can re-write the space and time derivatives in equation(2) as:

$$\frac{\partial}{\partial t} \left(\frac{\partial \phi}{\partial t} \right) = \left(\frac{\partial}{\partial t} + \frac{\partial}{\partial \tau} \frac{\partial \tau}{\partial t} \right) \left(\frac{\partial \phi}{\partial t} + \frac{\partial \phi}{\partial \tau} \epsilon^2 \right) = \frac{\partial^2 \phi}{\partial t^2} + 2\epsilon^2 \frac{\partial^2 \phi}{\partial \tau \partial t} + \frac{\partial^2 \phi}{\partial \tau^2} \epsilon^4 \quad (6)$$

with these equations, the EOM is given by:

$$\frac{\partial^2 \phi}{\partial t^2} + 2\epsilon^2 \frac{\partial^2 \phi}{\partial \tau \partial t} + \epsilon^4 \frac{\partial^2 \phi}{\partial \tau^2} - \epsilon^2 \frac{\partial^2 \phi}{\partial \rho^2} + \phi - \epsilon^2 \phi^3 + \Lambda \epsilon^2 \phi^5 = 0 \quad (7)$$

¹⁸The Hubble constant

to this equation, we consider the general solution in orders of ϵ of the form:

$$\phi = \epsilon(\phi_0 + \epsilon\phi_1 + \epsilon^2\phi_2 + \epsilon^3\phi_3 + \dots) \quad (8)$$

Equating equation(5) and solving for ϕ in the EOM, we are left with the corresponding equations of motion as:

$$\frac{\partial^2 \phi_0}{\partial t^2} + \epsilon \frac{\partial^2 \phi_1}{\partial t^2} + \epsilon^2 \frac{\partial^2 \phi_2}{\partial t^2} + 2\epsilon^2 \frac{\partial^2 \phi_0}{\partial \tau \partial t} - \epsilon^2 \frac{\partial^2 \phi_0}{\partial \rho^2} + \phi_0 + \epsilon\phi_1 + \epsilon^2\phi_2 + \Lambda\epsilon^2\phi_0^5 - \epsilon^2\phi_0^3 + \mathcal{O}(\epsilon^3) = 0 \quad (9)$$

With the above equation, we note that the zeroth order term in ϕ , is essentially a simple harmonic oscillator like term, with well studied solutions. Notice that we have safely separated the *actual space* x , and the *diluted space* ρ and we can now solve for in only the diluted space co-ordinates, but we still retain the *diluted time* coordinate τ with the actual time coordinate t . This is called the *two timing analysis*. Assuming the small value of ϵ , we can then count in powers of ϵ for the most prominent terms and safely neglect the higher order terms as $\epsilon < 1$, $\epsilon^2 \ll 1$ etc. For $\mathcal{O}(1)$ we are left with:

$$\frac{\partial^2 \phi_0}{\partial t^2} + \phi_0 = 0 \quad (10)$$

at $\mathcal{O}(\epsilon)$, we have:

$$\frac{\partial^2 \phi_1}{\partial t^2} + \phi_1 = 0 \quad (11)$$

for $\mathcal{O}(\epsilon^2)$, we then get:

$$\epsilon^2 \frac{\partial^2 \phi_2}{\partial t^2} + 2\epsilon^2 \frac{\partial^2 \phi_0}{\partial t \partial \tau} - \epsilon^2 \frac{\partial^2 \phi_0}{\partial \rho^2} + \epsilon^2 \phi_2 - \epsilon^2 \phi_0^3 + \Lambda\epsilon^2 \phi_0^5 = 0 \quad (12)$$

All the higher ordered terms in ϵ is sub-dominant due to its smallness. We now attempt to solve the partial differential equations involved to arrive at a general solutions for the relevant orders of magnitude equations. The general solution for ϕ_0 from equation(7) is then of the form:

$$\phi_0 = \frac{1}{2} (A(\rho, \tau)e^{-it} + A^*(\rho, \tau)e^{it}) \quad (13)$$

where A is a function of ρ and τ and A^* is the complex conjugate. Substituting this into equation(9), we could re-write the equation(9) into:

$$\epsilon^2 \frac{\partial^2 \phi}{\partial t^2} + \epsilon^2 \phi_2 = -2\epsilon^2 \frac{\partial^2 \phi_0}{\partial t \partial \tau} + \epsilon^2 \frac{\partial^2 \phi_0}{\partial \rho^2} + \epsilon^2 \phi_0^3 - \Lambda\epsilon^2 \phi_0^5$$

evaluating each term we get,

$$-2 \frac{\partial^2 \phi_0}{\partial t \partial \tau} = i(A_\tau e^{-it} - A_\tau^* e^{it})$$

$$\frac{\partial^2 \phi_0}{\partial \rho^2} = \frac{1}{2} (A_{\rho\rho} e^{-it} + A_{\rho\rho}^* e^{it})$$

$$\phi_0^3 = \frac{1}{8} (A e^{-it} + A^* e^{it})^3$$

Collecting all the relevant terms we then have the equation of the form:

$$\frac{A_{\rho\rho}}{2} + iA_\tau + \frac{3}{8}|A|^2 A = 0 \quad (14)$$

This mathematical treatment of the equations of motion is analogous to the physical system of a driven harmonic oscillator where the driver terms have to separately equate to zero. With the ansatz $A = a(\rho)e^{i\tau/2}$ we get:

$$a_{\rho\rho} - a + \frac{3}{4}a^3 = 0 \quad (15)$$

Looking at the tail end of the above equation, we note that the non-linearity of the potential is irrelevant and we are left with a small constant value at the tail ends of the potential with $V' \propto \phi$, we obtain the required boundary conditions:

$$\frac{d^2 a}{d\rho^2} - a = 0 \quad \text{for } \rho \gg 1, a \ll 1 \quad (16)$$

the general solution for a then is of the form:

$$a = C_1 e^\rho + C_2 e^{-\rho}$$

we take $\rho \rightarrow \infty$, we are led to the condition:

$$\frac{a_\rho}{a} = -1 \implies (a_\rho)_{\rho \rightarrow \infty} = -a_{\rho \rightarrow \infty}$$

if we assume that the trailing end of the envelope is an arbitrary constant κ , inline with all the above considerations, then:

$$a = \kappa \implies a_\rho = -\kappa$$

evaluating a at $\rho = 0$ then we are left with:

$$\rho = 0, a_\rho = 0$$

With these conditions we note that the oscillon potential with a quadratic minimum must necessarily satisfy $V'(\phi) < \phi$, for a given range of values. One of the relevant potential candidates maybe the QCD axions as mentioned in [1]. We can now use these conditions to break down second order ODE into a first order ODE by:

$$\frac{da}{d\rho} = b, \quad \frac{db}{d\rho} = a - \frac{3}{4}a^3 \quad (17)$$

with the initial conditions:

$$b(0) = 0, \quad b(\infty) = -\kappa$$

With the above conditions in place, it is straight forward to solve for the profile of $a(\rho)$. The calculated profile is then substituted back into the general solution for ϕ at $t = 0$ to get the equation of the form:

$$\phi = \epsilon a(\rho) \cos(\omega t) + \mathcal{O}(\epsilon^2) \quad (18)$$

where,

$$\omega = 1 - \frac{\epsilon^2}{2}$$

It is imperative to note that we have conveniently set the mass to unity due to the small ϵ parameter, otherwise there would be a mass factor in the expression for ω as mentioned in the previous discussions.

4 Computational details

Continuing from the last section, observing the equation(14) we see that this can be solved numerically by using various computational algorithms. One of the standard ways to solve non-stiff Initial value problems (IVPs) is to use the Runge-Kutta[3][4] method for solving ODEs.

4.1 The Runge-Kutta Method

Assuming previous knowledge of the Euler method for solving ODEs with initial conditions, we naturally extend to the Runge-Kutta (RK) methods which, achieve the accuracy of a Taylor series approach without requiring the calculation of higher derivatives. Inherently, the RK method exists with many variations exist and can be generalized into:

$$y_{i+1} = y_i + \phi(x_i, y_i, h)h \quad (19)$$

where ϕ is the increment function, which can be interpreted as a representative slope over the interval. The increment function can be written in general as:

$$\phi = a_1 k_1 + a_2 k_2 + \cdots + a_n k_n$$

where the a_i are constants and the k_n are given by:

$$\begin{aligned} k_1 &= f(x_i, y_i) \\ k_2 &= f(x_i + p_1 h, y_i + q_{11} k_1 h) \\ k_3 &= f(x_i + p_2 h, y_i + q_{21} k_1 h + q_{22} k_2 h) \\ &\vdots \\ k_n &= f(x_i + p_{n-1} h, y_i + q_{n-1,1} k_1 h + q_{n-1,2} k_2 h + \cdots + q_{n-1,n-1} k_{n-1} h) \end{aligned}$$

where the p 's and q 's are constants. The recurrence of the k 's in subsequent steps makes the RK method exceptionally efficient for computer calculations. Once the n is fixed, the values of the constants are evaluated by setting equation(15.) equal to terms in a Taylor series expansion. The local truncation error is $\mathcal{O}(h^3)$ and the global error is $\mathcal{O}(h^2)$. For our purposes, we will be using RK-4th order, the global truncation error is then $\mathcal{O}(h^4)$.

4.2 The Shooting method

In our current problem as described in previous sections, we see that the form of the ODE to be solved to study the oscillons fall under the category of boundary value problems (BVPs). This is because the conditions for the oscillon profile are specified at the extreme points or boundaries. A variety of significant physical processes fall within this class, but for our purposes we discuss here the shooting method for solving BVPs.

The shooting method is centered on converting the boundary-value problem into an equivalent initial-value problem. A trial-and-error approach is then implemented to solve the initial-value version. The equations require an initial value as input and the other values are guessed. The solution is then obtained by integrating using a fourth-order RK method with a suitable step size. We then obtain a value at the end of the interval. This value may differ from the boundary condition and therefore, another guess is made and the subsequent computation performed. This is continued until the boundary condition is met, in essence “shooting” until it hits the target boundary condition. This is the linear shooting method, based on the linearity in the subsequent guesses.

For non-linear boundary-value problems, linear interpolation or extrapolation through two solution points will not necessarily result in an accurate estimate of the required boundary condition to attain an exact solution. An alternative is to perform three iterations of the shooting method algorithm and use a quadratic interpolating polynomial to estimate the proper boundary condition. However, it is unlikely that such an approach would yield the exact answer, and additional iterations would be necessary to obtain the solution. This then leads us to formulate a different approach. With an iterative approach, we can efficiently find the amount of which the IVP fails to satisfy the boundary conditions. In a two point BVP, this corresponds to the value at $x = b$. We are then interested in the amount by which $y(b, \lambda)$ misses the target condition β . The non-linear shooting method is then finding an approximate root λ^* of $F(\lambda)$ by solving:

$$F(\lambda) = y(b, \lambda) - \beta = 0 \quad (20)$$

The above equation computationally expensive as each value of $F(\lambda)$ is calculated by numerically by solving an IVP, and hence a method that rapidly leads to convergence is ideally used. Some of the methods used in this respect are bisection method, secant method, Newton's method, etc.

4.2.1 The Secant method[5]

Although Newton's method is the fastest to converge, in many problems, we do not have analytic solutions for $F(\lambda)$. The Secant method is then ideal for such conditions. We first make two guesses for solving equation(20) by choosing appropriate λ_0 and λ_1 . Then we solve the IVPs and find the corresponding F 's. The third guess then is supplied by the formula:

$$\lambda_2 = \lambda_1 - \left(\frac{\lambda_1 - \lambda_0}{F(\lambda_1) - F(\lambda_0)} \right) F(\lambda_1) \quad (21)$$

The above formula can be iteratively used to generate λ 's until convergence. One of the curial steps is then the choice of the initial guesses.

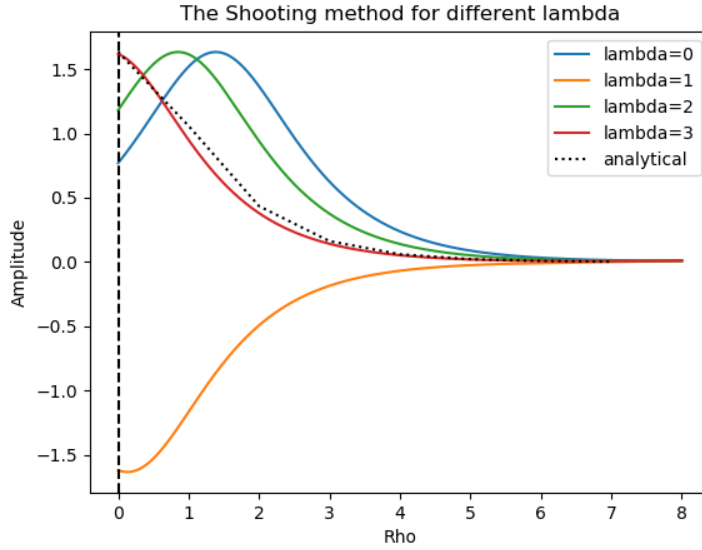


Figure 4: The shooting method applied for the oscillon problem. The recursive secant algorithm is clearly apparent by the various λ values being plotted.

4.3 Finite differencing

With the numerical solution of the oscillon profile in hand, we are now equipped to calculate the energy of the oscillon thus formed. To verify the oscillon profile that is obtained, we substitute it into the EOM and check if it is satisfied. The derivatives w.r.t time and space are found by using the forward finite difference method, as:

$$\dot{\phi}(t, x) = \frac{\phi(t + \Delta t) - \phi(t)}{\Delta t}$$

$$\ddot{\phi}(t, x) = \frac{\phi(t + 2\Delta t) - 2\phi(t + \Delta t) + \phi(t)}{(\Delta t)^2}$$

And for space, similarly we use the central finite difference method:

$$\begin{aligned}\frac{d\phi}{dx}(t, x) &= \frac{\phi(x + \Delta x) - \phi(x - \Delta x)}{2\Delta x} \\ \frac{d^2\phi}{dx^2}(t, x) &= \frac{\phi(x + \Delta x) + \phi(x - \Delta x) - 2\phi(x)}{(\Delta x)^2}\end{aligned}$$

5 Oscillon Energy and time evolution

From scalar field theory and from the above discussions, it is evident that the calculation of the energy and the time evolution of the system is intimately related to calculating the Hamiltonian density of the system, given by:

$$\mathcal{H} = \frac{1}{2} ((\Pi^2 + (\partial_x \phi)^2)) + V(\phi) \quad (22)$$

where Π is the canonical momentum density which is nothing but $\partial_t \phi$ in our case. For the energy we then integrate the Hamiltonian density to obtain

$$E = \int \left(\frac{1}{2} (\partial_t \phi)^2 + \frac{1}{2} (\partial_x \phi)^2 + \frac{m^2 \phi^2}{2} - \frac{\phi^4}{4} \right) dx \quad (23)$$

Calculating each term for the energy equation, we find:

$$\frac{1}{2} (\partial_t \phi)^2 = \frac{1}{2} \epsilon^2 a^2(\rho) \sin^2(\omega t) + \mathcal{O}(\epsilon^2)$$

similarly for the spatial part:

$$\frac{1}{2} (\partial_x \phi)^2 = \frac{1}{2} \epsilon^2 \cos^2(\omega t) \left(\frac{da}{dx} \right)^2 = \frac{1}{2} \epsilon^4 \left(\frac{da}{d\rho} \right)^2 \cos^2(\omega t)$$

for the mass term we have:

$$\frac{m^2 \phi^2}{2} = \frac{m^2 \epsilon^2}{2} a^2(\rho) \cos(\omega t)$$

and for the ϕ^4 term, we have:

$$\frac{\phi^4}{4} = \frac{\epsilon^4}{4} \cos^4(\omega t)$$

we now note that all the terms except the mass term and the partial derivative w.r.t time, all are of $\mathcal{O}(\epsilon^4)$ and are therefore subdominant. The energy equation is then further reduced to:

$$E = \int \frac{1}{2} \epsilon^2 a^2(\rho) (\sin^2(\omega t) + m^2 \cos^2(\omega t)) dx \quad (24)$$

note that $m = \omega$, and for smaller values of ϵ , ω tends to unity. This is then a convenient choice here and the change of variables with $dx = d\rho/\epsilon$, the equation then becomes:

$$E = \frac{\epsilon}{2} \int a^2(\rho) d\rho$$

Continuing from equation(2), from the equations of motion, for the oscillon evolution equation, we have:

$$\frac{d^2\phi}{dt^2} = \frac{d^2\phi}{dx^2} - \phi + \phi^3 - \frac{\phi^5}{\epsilon^2}$$

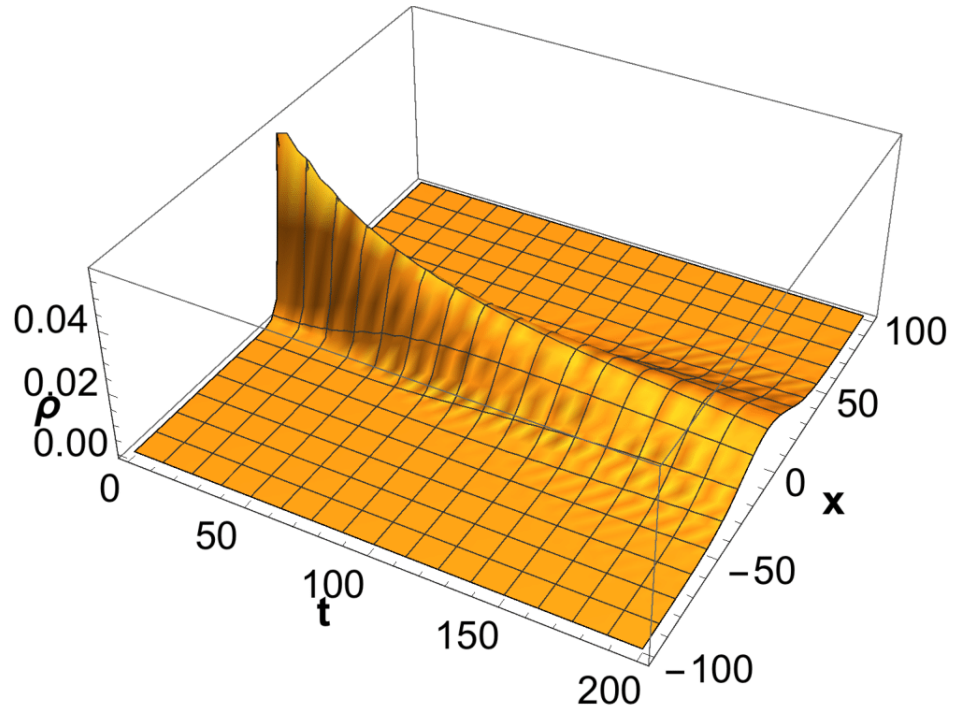
where we have normalised the Λ parameter to unity. Substituting the finite differencing approximations for the derivatives in the equation of motion, we get:

$$\frac{\phi(t + \Delta t) - 2\phi(t) + \phi(t - \Delta t)}{(\Delta t)^2} = \frac{\phi(x + \Delta x) + \phi(x - \Delta x) - 2\phi(x)}{(\Delta x)^2} - \phi + \phi^3 - \frac{\phi^5}{\epsilon^2}$$

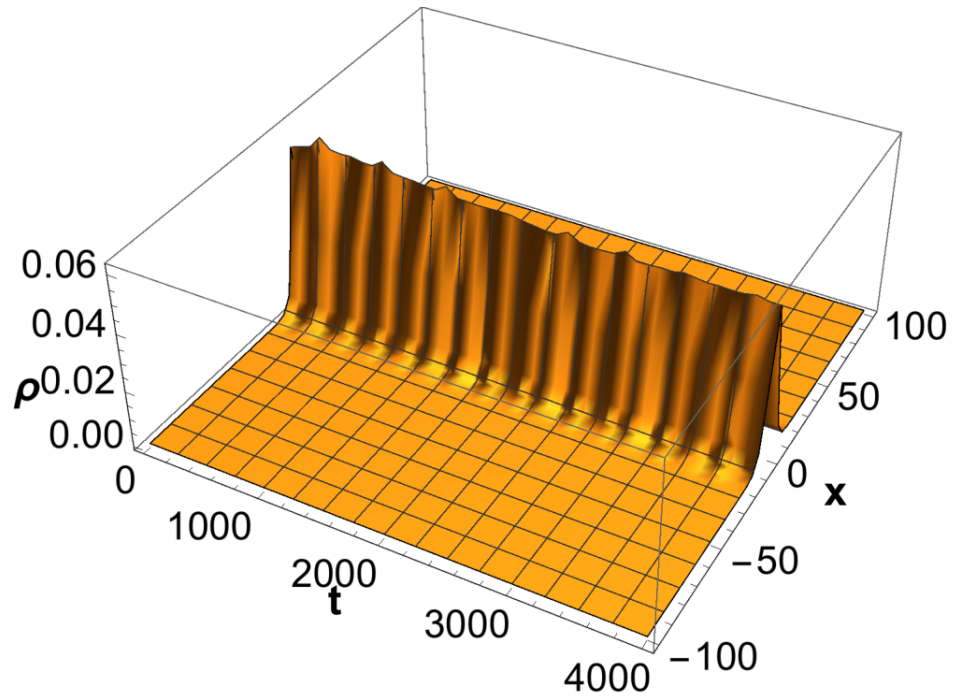
$$\phi(t + \Delta t) - 2\phi(t) + \phi(t - \Delta t) = \left(\frac{\phi(x + \Delta x) + \phi(x - \Delta x) - 2\phi(x)}{(\Delta x)^2} - \phi + \phi^3 - \frac{\phi^5}{\epsilon^2} \right) (\Delta t)^2$$

$$\phi(t + \Delta t) = \left(\frac{\phi(x + \Delta x) + \phi(x - \Delta x) - 2\phi(x)}{(\Delta x)^2} - \phi + \phi^3 - \frac{\phi^5}{\epsilon^2} \right) (\Delta t)^2 + 2\phi(t) - \phi(t - \Delta t) \quad (25)$$

with the above equation, we calculate the time evolution of our system.



(a) Here we see the linear solutions for the equations in our previous discussions. The field is clearly dissipative and no oscillons are formed.



(b) Here we see the persistence of the wave solution for times $\sim \mathcal{O}(10^3)$. This is only achieved by the non linearities in the potential

6 Multicomponent oscillon models:

Our previous discussions dealt with the theory of single scalar oscillon fields and the simulation of the same. Various numerical methods were also discussed. The natural extension to the central question of this work is to study the dynamics and characteristics of multi component oscillon fields. As stated in section 3, we see that this question is not without its own set of motivations. A large number of scalar fields or moduli fields arise in the context of String theories and other *Grand Unification theories*¹⁹. Moreover the highly successful Standard Model theory which is the QFT describing the building blocks of matter, is made up of many fields. Based on these considerations, we mention here the various multi-component scenarios discussed in the context of oscillons.

The simplest method to study oscillon formation in this investigative scenario is to use a toy model of a well studied theory (like the SM for instance) and apply the oscillon conditions for the same. One of the prominent such models is the $SU(2)$ added with the Higg's field[2, 56, 55, 57]. This electro-weak (EW) oscillon scenario is very favourable for the study of oscillons as this is easily scalable to include the strong interactions and invariably incorporate the full symmetry group of the SM. As with incorporating larger number of fields, the electro weak investigations get highly tedious with the increased degrees of freedom in the gauge field. It is then highly advantageous to follow through the calculations with the spherical ansatz[2, 56, 57] which leave the Lagrangian invariant under the combined rotations in normal 3D space and the isospin space. As no symmetry is assumed in this setup, the $U(1)$ hypercharge can also be incorporated into our calculations. It is also imperative to note that the EW oscillon field follows the linear dispersion relations at their extrema (high field values)[55].

With the given EW oscillon setup, numerical simulations were carried out in a similar fashion as to the one performed in this work. The results lead us to a peculiar resonant condition that the Higg's mass and the W mass must be in the ratio 2 : 1, necessary for oscillon formation [57, 55, 59]. The studies also show that the resultant oscillon stays stable for $\sim 10^3$ oscillations[59]. This is contrary to what one would naively expect, as an increased number of fields may result in increased decay pathways, but that is not the case here. The formed oscillon initially decays into the massless field, but as it evolves in time, it gradually settles to a neutral configuration where the coupling to the massless field is highly suppressed[55, 57]. Although the studied oscillons seem to be stable for long periods of time, there is also a possibility of decay through non spherical effects[59]. Due to their stability it is plausible that the oscillons may have played an important role in the early universe such as sourcing the necessary out of equilibrium conditions (slow decay[55]) for baryogenesis[59]. They are also excellent dark matter candidates, due to them behaving as energy sinks.

Another approach in studying oscillon formation in multiple fields is the use

¹⁹theories that try to unify the fundamental forces of nature.

of hybrid inflation theories. In [58], the investigative model includes two fields, coupled in a four-point interaction vertex of a Feynman diagram with potentials from hybrid inflation theories. We see that the description is in contrast with the $SU(2)$ based studies, and leads to increased oscillon lifetimes which are at least four times the ones observed in the $SU(2) + higgs$ model. This maybe be because of the peculiar two state formation of this *hybrid oscillon* model and the periodic transition between the two. These higher lifetimes can very well be of importance during the post inflation era, as they can significantly trap energy from the primordial plasma, and lead to various deviations from equilibrium conditions. It is thus imperative that the search of non-linearities in the theories surrounding the early universe must be perused, as they may have the answers to some of the pressing questions of Cosmology and maybe even for all of Physics.

A Quantum Mechanical operators[?, 41]:

x-component of momentum:

$$P_x \rightarrow \frac{\hbar}{i} \frac{\partial}{\partial x}$$

Time-independent Hamiltonian with a potential $V(x)$:

$$E \rightarrow \frac{P^2}{2m} + V(x)$$

Time-dependent Hamiltonian:

$$E \rightarrow i\hbar \frac{\partial}{\partial t}$$

Kinetic Energy:

$$KE \rightarrow \frac{-\hbar^2}{2m} \frac{\partial^2}{\partial x^2}$$

Time evolution operator:

$$\hat{U} = e^{-i\hat{H}t/\hbar}$$

Parity Operator:

$$\hat{P}\psi(r) = \psi(-r)$$

Ladder operators for a quantum mechanical simple harmonic oscillator:

$$a^\dagger = \sqrt{\frac{m\omega}{2\hbar}} \left(x - i \frac{\hat{p}}{m\omega} \right)$$
$$a = \sqrt{\frac{m\omega}{2\hbar}} \left(x + i \frac{\hat{p}}{m\omega} \right)$$

B Euler-Lagrange equation[42]:

The Euler-Lagrange(EL) equation is one of the most important equations in all of physics and mathematics, especially in relation to the calculus of variations. The EL equation is the differential equation that a smooth, continuous function satisfies while trying to minimize path between two stationary points. Analytically it can be stated as: Given a continuous and smooth function $y(x)$, minimizing the integral:

$$I = \int_{x_1}^{x_2} f(x, y, y') dx$$

what is the equation that $y(x)$ must satisfy, given x_1, x_2, y_1 and y_2 . Let us assume that $y(x)$ is *not* such a function per say and construct a *comparison* function $Y(x)$ such that:

$$Y(x) = y(x) + \alpha\eta(x)$$

where η is an arbitrary function satisfying:

$$\eta(x_1) = \eta(x_2) = 0$$

and α is the parameter of the family of lines. We can think of this as two families of connecting two points in the xy plane at (x_1, y_1) and (x_2, y_2) and η is a parameter of deviation of Y family of lines to the y family of lines. Substituting our new family of curves into the integral above we get:

$$I(\alpha) = \int_{x_1}^{x_2} f(x, Y, Y') dx$$

At the boundaries of the two points in the xy plane, the first derivative w.r.t α for the above integral must vanish as Y and y are same at the stationary end points. Thus we have:

$$I'(0) = 0$$

$$I'(\alpha) = \int_{x_1}^{x_2} \left(\frac{\partial f}{\partial Y} \frac{\partial Y}{\partial \alpha} + \frac{\partial f}{\partial Y'} \frac{\partial Y'}{\partial \alpha} \right) dx = \int_{x_1}^{x_2} \left(\frac{\partial f}{\partial Y} \eta + \frac{\partial f}{\partial Y'} \eta' \right) dx$$

evaluating the above integral at $\alpha = 0$, with an equivalent replacement from Y to y we have:

$$I'(0) = \int_{x_1}^{x_2} \left(\frac{\partial f}{\partial y} \eta + \frac{\partial f}{\partial y'} \eta' \right) dx = 0$$

using integration by parts, we get:

$$I'(0) = \int_{x_1}^{x_2} \left[\frac{\partial f}{\partial y} - \frac{\partial}{\partial x} \left(\frac{\partial f}{\partial y'} \right) \right] \eta dx = 0$$

as η is an arbitrary function, this equation must hold true for all η , we arrive at the *Euler-Lagrange* equation:

$$\frac{\partial f}{\partial y} - \frac{\partial}{\partial x} \left(\frac{\partial f}{\partial y'} \right) = 0$$

C Cosmic Inflation:

In the year 1915, Albert Einstein published his magnum opus, the theory of *General Relativity*. The fairly controversial theory pointed out that space and time were not two separate quantities but one and the same entity called *spacetime* and that gravity was the result of curvature of this spacetime fabric. While the scientific community debated on the validity of the theory, a Belgian priest, Georges Le-maitre was intrigued by the Einstein field equations and proposed a theory of an ever expanding universe which started from a point of singularity[45]. This theory came to be known as the *Big bang* theory (BBT) and was validated by the pioneering work on observational Astronomy by Edwin Hubble[46]. It has since become a standard theory of modern cosmology.

According to the BBT, after about 380 000 years from the initial singularity, the universe had cooled enough to allow the formation of the first hydrogen atoms. During this process, the photons decoupled from the primordial plasma and started free streaming into the expanding universe[49]. This highly red-shifted radiation is called the *cosmic microwave background* (CMB) and is one of the most precisely measured spectrum in all of nature[47]. The CMB radiation is thus the oldest form of radiation that can be measured by the telescopes on earth, implying that if we were to look at a patch of the CMB in one particular direction, the spectrum should be highly different from a similar patch of the CMB located at 180° with respect to the first patch, as the light from these two patches should not have had enough time to interfere with each other. But the observations of the CMB point otherwise. The temperature of the CMB is fairly uniform with an uncertainty of about 0.0001K[48]. This inconsistency between the actual age of the universe and the homogeneity of the CMB is referred to as the *Horizon problem*.

Alan Guth, a theoretical physicist at the Cornell University came up with an ingenious explanation to account for the horizon problem. He argued that after the initial singularity of the big bang, the Universe went through a period of rapid exponential spatial expansion before reheating and forming the structures we see today. He coined the term *inflation* for the rapidly expanding regime and the driver of this expansion, the *inflaton* field. Apart from solving the horizon problem, this theory could correctly account for the flatness of the observable universe and even allow us to calculate the quantum fluctuations of the primordial plasma[50].

D Tests on the Runge-Kutta method:

As with all other conventional experiments, we can only make justified scientific conclusions and discoveries based on the accuracy of the experimental apparatus in question. It is then imperative and all the more essential to use convergence tests on computational algorithms that are being used. To this effect, the algorithm was tested by solving a simple partial differential equation, given by:

$$\frac{dy}{dx} = -2x^3 + 12x^2 - 20x + 8.5$$

with the exact solution:

$$y = -0.5x^4 + 4x^3 - 10x^2 + 8.5x + 1$$

The following result was obtained as required.

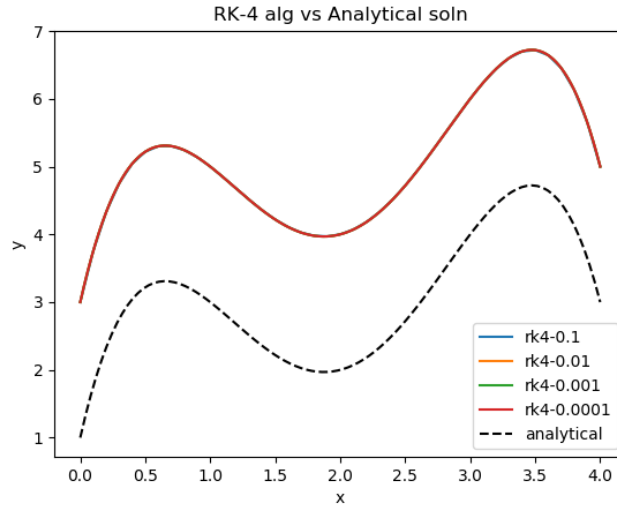


Figure 5: The Runge-Kutta algorithm plotted against the analytical solution with decreasing step sizes

The global errors were also plotted with respect to the analytical solution

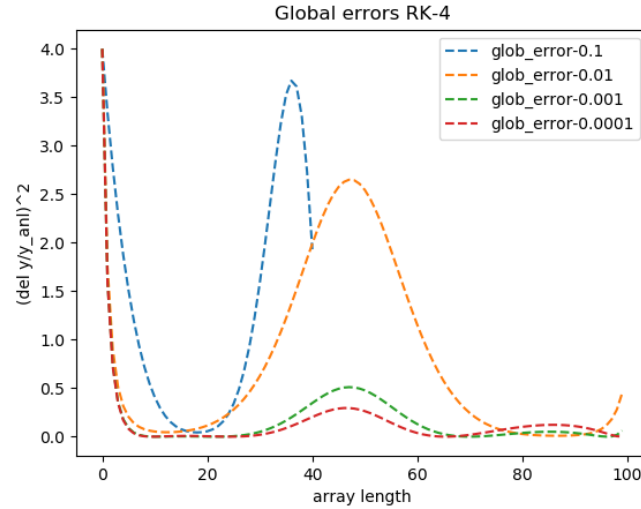


Figure 6: The global errors calculated with decreasing step size using the RK algorithm

D.1 The source-code used:

This source-code is written in Python 3+

```
import matplotlib.pyplot as plt
import numpy as np

# functions for inegration:
def integrator(x,y,h,xend,alg):
    # integrator routine
    while (x<xend):
        if ((xend-x)<h):
            h = xend -x
        if alg == 'rk4':
            x,ynew = rk4(x,y,h)
            y = ynew
    return x,y

def derivatives(x,y):
    "returns dy/dx at given x and y"
    dydx = -2*x**3 + 12*x**2-20*x+8.5
    return dydx

def driver(x_init,x_final,dx,xout,y,alg):
    "driver function"
```

```

x = x_init
x_arr = []
y_arr = []
x_arr.append(x)
y_arr.append(y)
m = 0
while x < x_final:
    if abs(dx) > abs(xout):
        print("fine graining cannot be greater
              than coarse graining, exiting the loop...")
        break
    xend = x + xout
    if xend > x_final:
        print("step size from x to the next x is
              too big, defaulting to xend = ", x_final)
        xend = x_final
    h = dx
    if m == 0:
        print("estimated number of integrator loops = ", round(xend/h))

    x, y = integrator(x, y, h, xend, alg)
    m += 1
    if x > x_final:
        print("value of calculated x exceeds limit, exiting...")

        break
    x_arr.append(x)
    y_arr.append(y)
return x_arr, y_arr, m

def rk4(x, y, h):
    "uses RK 0(4) method algorithm to calculate the next step "
    k1 = derivatives(x, y)
    ym = y + k1*(h/2)
    k2 = derivatives(x+(h/2), ym)
    ym = y + k2*(h/2)
    k3 = derivatives(x+(h/2), ym)
    ye = y + k3*h
    k4 = derivatives(x+h, ye)
    slope = (k1 + 2*(k2 + k3) + k4)/6
    ynew = y + slope*h
    x = x+h
    return x, ynew

```



```

if __name__ == "__main__":

    # initialization
    y = 1.# initial value of dependant variable
    x_init = 0.# initial value of independant variable
    x_final = 4.# final value of independant variable
    dx = 1e-1 # step size within the interval from one
               x to the next (fine graining)
    xout = 1e-1 #step size for the next value of x (coarse graining)
    method3 = 'rk4'
    x3,y3,m3 = driver(x_init,x_final,dx,xout,y,method3)
    x_anl = np.linspace(0,4,100)
    y_anl = []

    for i in x_anl:

        y=-0.5*i**4+ 4*i**3 - 10*i**2 + 8.5*i + 1
        y_anl.append(y)
    while dx>1e-5:
        x3,y3,m3 = driver(x_init,x_final,dx,xout,y,'rk4')
        glob_error = [(i-j)**2/i**2 for i,j in zip(y_anl,y3)]
        plt.plot([i for i in range(len(glob_error))],
                  glob_error,label='glob_error-{}'.format(dx),linestyle='--')

        dx /=10
        xout /=10
    #plotting
    #plt.plot(x_anl,y_anl,label = 'analytical',color='k',linestyle='--')

    plt.xlabel('x')
    plt.ylabel('y')
    plt.legend()
    plt.show()

```

E Testing the shooting method:

The shooting method is a numerical method for solving differential equations. Auxillary conditions, such as given values of the PDE at the begining and (or) the start of the interval of integration are used in evaluating the constant of integration for arriving at the final solution for the PDE. When conditions are specified at the begining of the integration limit, such problems are called *initial value problems* or IVPs. On the other hand, when these conditions are specified at the extrema of the system in question, they then constitute what is called a *boundary value problem* or BVPs. The shooting method is then a technique applied to BVPs, converting them into IVPs for obtaining their solutions. The system is then solved self-consistently through a trial and error approach to arrive at the final solution²⁰.

The shooting method used in this work was tested on a simple non-linear problem given by:

$$\frac{d^2y}{dx^2} = 2y^3$$

with boundary conditions: $y(1) = 0.25, y(2) = 0.2$ with x ranging from $(1, 2)$. With the formulation given in sub-section 4.2, we have:

$$F(\lambda) = y(b, \lambda) - \beta = y(2, \lambda) - 0.2$$

where $a = 1$, $b = 2, \alpha = 0.25$ and $\beta = 0.2$, the equivalent IVP is then:

$$\frac{dy_1}{dx} = y_2 \quad y_1(1) = 0.25$$

$$\frac{dy_2}{dx} = 2y_1^3 \quad y_2(1) = \lambda$$

where $y_1 = y$ and $y_2 = y'$ with the initial guess $\lambda_0 = (\beta - \alpha)/(b - a) = -0.05$, for our particular problem. The problem was solved in going from $\beta \rightarrow \alpha$ and vice versa, however only the former will be discussed here as it is the current one used.

The following result was obtained.

²⁰cf. sub-section 4.2

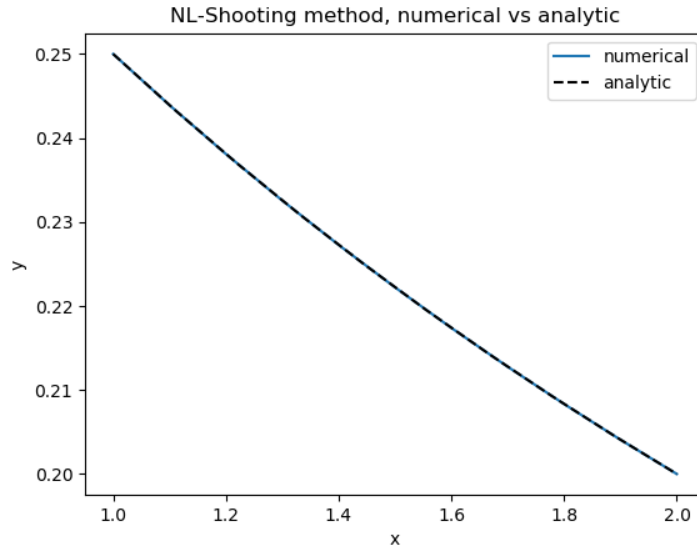


Figure 7: The non linear shooting method solutions for the given problem. There is a clear correlation between numerical and analytic solutions.

E.1 The source-code used:

The source-code is written in Python 3+

```
# functions for integration:
def integrator(x,y1,y2,h,xend,alg):
    "integrator routine"
    while (x>xend):
        if (abs(xend-x)<abs(h)):
            h = xend-x
        if alg == 'rk4':
            x,ynew1,ynew2 = rk4(x,y1,y2,h)
            y1 = ynew1
            y2 = ynew2
    return x,y1,y2

def derivatives(x,y1,y2):
    "returns dy/dx at given x and y"
    dydx1 = y2
    dydx2 = 2*y1**3
    return dydx1,dydx2

def driver(x_init,x_final,dx,xout,y1,y2,alg):
    "driver function"
```

```

x = x_init
x_arr = []
y_1_arr = []
y_2_arr = []
x_arr.append(x)
y_1_arr.append(y1)
y_2_arr.append(y2)
m = 0
while x > x_final:
    if abs(dx) > abs(xout):
        print("fine graining cannot be greater than coarse graining,
exiting the loop...")
        break
    xend = x + xout
    if xend < x_final:
        print("step size from x to the next x is too big, defaulting
to xend = ", x_final)
        xend = x_final
    h = dx
    if m == 0:
        print("estimated number of integrator loops = ", round(xend/h))
    x, y1, y2 = integrator(x, y1, y2, h, xend, alg)
    m = m + 1
    if x < x_final:
        print("value of calculated x exceeds limit, exiting...")

        break
    x_arr.append(x)
    y_1_arr.append(y1)
    y_2_arr.append(y2)
return x_arr, y_1_arr, y_2_arr, m

# functions defining ode solving methods:
def rk4(x, y1, y2, h):
    "uses Runge Kutta 0(4) method algorithm to calculate the next step"

    k1_1, k1_2 = derivatives(x, y1, y2)
    ym1 = y1 + k1_1*(h/2)
    ym2 = y2 + k1_2*(h/2)
    k2_1, k2_2 = derivatives(x+(h/2), ym1, ym2)
    ym1 = y1 + k2_1*(h/2)
    ym2 = y2 + k2_2*(h/2)
    k3_1, k3_2 = derivatives(x+(h/2), ym1, ym2)
    ye1 = y1 + k3_1*h
    ye2 = y2 + k3_2*h

```

```

        k4_1,k4_2 = derivatives(x+h,ye1,ye2)
        slope1 = (k1_1 + 2*(k2_1 + k3_1) + k4_1)/6
        slope2 = (k1_2 + 2*(k2_2 + k3_2) + k4_2)/6
        ynew1 = y1 +slope1*h
        ynew2 = y2 +slope2*h
        x = x+h
        return x,ynew1,ynew2

# shooting method functions
def shoot(lam,beta):
    f = (lam - beta)
    return f

def calc_lam(alpha,beta,x_init,x_final,dx,xout,n):
    lam = []
    f= []
    for i in range(n):
        try:
            if i ==0:
                lam0 = (beta-alpha)/(x_final-x_init)
                y2 = lam0
                y1 = alpha
                x,y1sol,y2sol,m = driver(x_init,x_final,dx,xout,y1,y2,'rk4')

                f0 = shoot(y1sol[-1],beta)
                lam.append(lam0)
                f.append(f0)
            if i ==1:
                lam1 = float(10*lam[-1])
                y2 = lam1
                y1 = alpha
                x,y1sol,y2sol,m = driver(x_init,x_final,dx,xout,y1,y2,'rk4')

                f1 = shoot(y1sol[-1],beta)
                lam.append(lam1)
                f.append(f1)
            if i>1:
                lam2 = lam[-1]-(lam[-1]-lam[-2])*f[-1]/(f[-1]-f[-2])
                y2 = lam2
                y1 = alpha
                x,y1sol,y2sol,m = driver(x_init,x_final,dx,xout,y1,y2,'rk4')

                f2 = shoot(y1sol[-1],beta)
                lam.append(lam2)
                f.append(f2)
        except ArithmeticError:
            break

```

```

        return lam,f,x,y1sol,y2sol,m
if __name__ == "__main__":
# initialization
    x_init = 2.# initial value of independant variable
    x_final = 1.# final value of independant variable
    dx = -0.1 # fine graining
    xout = -0.1
    alpha= 0.2 #shooting initial condition
    beta = 0.25 # shooting final condition
#shooting
    step = 100 # number of shooting steps
    lam,f,x,y1,y2,m = calc_lam(alpha,beta,x_init,x_final,dx,xout,step)

#plotting
    x_anal = np.linspace(0,2,10)
    y_anal = [1/(i+3) for i in x_anal]
    plt.plot(x,y1,label='numerical')
    plt.plot(x_anal,y_anal,label = 'analytic')
    plt.legend(loc='upper right')
    plt.show()

```

F The source code used for this work:

The source code is divided into two parts, one for finding the oscillon profile and the other concerns with its evolution. The initial sketches of the code were written in python, but with respect to the evolution golang was used as it was found to be faster.

F.1 Oscillon profile:

```
#!/bin /python
""" This code attempts to solve the relevant equations for a single
field Oscillon
This code is written in Python 3
Author: Athul Muralidhar
Date: 10 May 2018
Due credits given to S.Evangelos for his guidance and utmost patience,
and helping the author with the code
"""
# initial imports:
from matplotlib import pyplot as plt
import math

# functions for integration:
def driver(x_init,x_final,dx,xout,y1,y2):
    "driver function"
    x = x_init
    x_arr = []
    y_1_arr = []
    y_2_arr = []
    x_arr.append(x)
    y_1_arr.append(y1)
    y_2_arr.append(y2)
    while x>x_final:
        if abs(dx)>abs(xout):
            break
        xend = x + xout
        if xend<x_final:
            xend = x_final
        h = dx
        x,y1,y2 = integrator(x,y1,y2,h,xend)
        if x < x_final:
            break
        x_arr.append(x)
        y_1_arr.append(y1)
        y_2_arr.append(y2)
    return x_arr,y_1_arr,y_2_arr
```

```

def integrator(x,y1,y2,h,xend):
    "integrator routine "
    while (x>xend):
        if (abs(x-xend)<abs(h)):
            h = (xend-x)
            x,ynew1,ynew2 = rk4(x,y1,y2,h)
            y1 = ynew1
            y2=ynew2
    return x,y1,y2

def derivatives(x,y1,y2):
    "returns dy/dx at given x and y"
    dydx1 = y2
    dydx2 = y1 - (3/4)*y1**3
    return dydx1,dydx2

# functions defining ode solving methods:
def rk4(x,y1,y2,h):
    "uses Runge Kutta 0(4) method algorithm to calculate the next step"

    k1_1,k1_2 = derivatives(x,y1,y2)
    ym1 = y1 + k1_1*(h/2)
    ym2 = y2 + k1_2*(h/2)
    k2_1,k2_2 = derivatives(x+(h/2),ym1,ym2)
    ym1 = y1 + k2_1*(h/2)
    ym2 = y2 + k2_2*(h/2)
    k3_1,k3_2 = derivatives(x+(h/2),ym1,ym2)
    ye1 = y1 + k3_1*h
    ye2 = y2 + k3_2*h
    k4_1,k4_2 = derivatives(x+h,ye1,ye2)
    slope1 = (k1_1 + 2*(k2_1 + k3_1) + k4_1)/6
    slope2 = (k1_2 + 2*(k2_2 + k3_2) + k4_2)/6
    ynew1 = y1 +slope1*h
    ynew2 = y2 +slope2*h
    x = x+h
    return x,ynew1,ynew2

# shooting method functions
def shoot(lam,beta):
    f = lam - beta
    return f

def calc_lam(alpha,beta,x_init,x_final,dx,xout,n):
    lam = []
    f= []
    for i in range(n):
        try:
            if i ==0:

```



```

        lam0 = (beta-alpha)/(x_final-x_init)
        y2 = lam0
        y1 = alpha
        x,y1sol,y2sol = driver(x_init,x_final,dx,xout,y1,y2)

        plt.plot(x,y1sol,label='kappa-0')
        f0 = shoot(y1sol[-1],beta)
        lam.append(lam0)
        f.append(f0)
    if i ==1:
        lam1 = float(10*lam[-1])
        y2 = lam1
        y1 = alpha
        x,y1sol,y2sol = driver(x_init,x_final,dx,xout,y1,y2)
        plt.plot(x,y1sol,label='kappa-1')
        f1 = shoot(y1sol[-1],beta)
        lam.append(lam1)
        f.append(f1)
    if i>1:
        lam2 = lam[-1]-(lam[-1]-lam[-2])*f[-1]/(f[-1]-f[-2])

        y2 = lam2
        y1 = alpha
        x,y1sol,y2sol= driver(x_init,x_final,dx,xout,y1,y2)

        plt.plot(x,y1sol,label = 'kappa-{}'.format(i))

        f2 = shoot(y1sol[-1],beta)
        lam.append(lam2)
        f.append(f2)
    except ArithmeticError:
        break
    return lam,f,x,y1sol,y2sol

if __name__ == "__main__":
    # initialization
    x_init = 7. # initial value of independant variable
    x_final = 0. # final value of independant variable
    dx = -0.01 # fine graining
    xout = -0.01
    alpha= 0.01 #shooting initial condition
    beta = 0.0 # shooting final condition
    #shooting
    step = 100 # number of shooting steps
    lam,f,x,y1,y2 = calc_lam(alpha,beta,x_init,x_final,dx,xout,step)
    #plotting

```

```

x_anal = [i for i in range(8)]
y1_anal = [2*math.sqrt(2/3)*1/math.cosh(i) for i in x_anal]
plt.plot(x_anal,y1_anal,color = 'k', label = 'analytical')
plt.xlabel('rho')
plt.ylabel("y1")
plt.title('distance vs a for different kappa values')
plt.legend(loc = 'upper right')
plt.axvline(x=0, color = 'k', linestyle = '--')
plt.tight_layout()
# plt.savefig('rhovsadiiffkappa')
plt.show()
# writing to text file
with open('stdout.txt','w') as file:
    file.write('x y1 y2\n')
    for i in range(len(x)):
        file.write('{} {} {} \n'.format(x[i],y1[i],y2[i]))

```

F.2 Oscillon evolution:

As afore mentioned the initial sketches of the oscillon profile was written in Python 3 while the up-scaled version is in goolang. Both are provided here as reference.

F.2.1 Python version

```

#!/bin/ python
""" This source code aims to evolve the Oscillon profile from the
analytical solution.
This code is written in Python 3
Author: Athul Muralidhar
Date: 06 June 2018
Due credits given to S.Evangelos for his guidance and utmost patience,
and helping the author with the code
avg time: 0.081593796 sec with min time and space steps
"""

# initial imports
import matplotlib.pyplot as plt
import math import numpy as np
from time import time

def frange(start,stop, step=1.0):
    while start < stop:
        yield start
        start +=step

if __name__ == '__main__':
#initial Conditions

```

```

s=time()
dx = 0.1 #coordinate distance
dt = 0.1*dx #coordinate time
eps = 0.1
timesteps=int(1//dt)
x_steps = int(1//dx)
E_init=0
Eevol=np.zeros(timesteps,dtype=np.float)
TS1=[]
phi_at_x = []
omega = 1-0.5*eps**2
nl=0
# analytical oscillon solution
a=[2*math.sqrt(2/3)*1/np.cosh(i*eps) for i in frange(-x_steps,x_steps+1,dx)]

a[0]=0
a[-1] = 0
TS1=[i*eps for i in a]
TS1=np.asarray(TS1)
len_TS = len(TS1)
TS2=np.zeros(len_TS,dtype=np.float)
phi_at_x.append(TS1[len_TS//2])
plt.plot([i for i in frange(-x_steps,x_steps+1,dx)],TS1,label='phi
at init',color='k',linestyle='--')
E_init=0
for i in TS1:
    E_init +=0.5*dx*i**2

#time evolution - eom calculation
for i in range(len_TS-1):
    TS2[i]=TS1[i]
    for t in range(timesteps+1):
        TS3=np.zeros(len_TS,dtype=np.float)
        E=0
        for i in range(len_TS-2):
            if i == 0:
                TS3[i]=0.0
                continue
            phi_xx = (TS2[i+1]+TS2[i-1]-2*TS2[i])/dx**2
            phievol = (phi_xx - TS2[i] + nl*TS2[i]**3 - nl*TS2[i]**5/eps**2
)*dt**2 + 2*TS2[i]-TS1[i]
            TS3[i]=phievol
            E+=(0.5*((TS3[i]-TS2[i])/dt)**2 + 0.5*((TS2[i+1]-TS2[i])/dx)**2
+ 0.5*TS2[i]**2 -nl*0.25*TS2[i]**4)*dx
        TS3[len_TS-1]=0
        phi_at_x.append(TS2[len_TS//2])
        for i in range(len_TS-1):

```

```

        TS1[i]=TS2[i]
        TS2[i]=TS3[i]
    E1=E
    Eevol.append(E1)

#plotting and printing
    if t%10==0:
        Eevol.append(E1)
        print('TS1:',TS1)
        print('\nTS2:',TS2)
        print('\nTS3:',TS3)
        plt.plot([i for i in range(-rho_steps,rho_steps+1)],TS2,label='phi
at t={}'.format(t))
        plt.plot([i for i in range(-rho_steps,rho_steps+1)],TS3,label='phi
at t={}'.format(t))

    e = time()
    print('time taken:{}'.format(e-s))
    plt.axhline(y=0,color='k')
    plt.legend(loc = 'upper left',prop={'size': 8})
    plt.legend()
    plt.show()

```

F.2.2 Go version:

```

// this source code is compatible with the osc_evol_np.py source
code using numpy implimentation
// in Python. This is the gophered version of the program implimentation.
The implimentation is
// consistant completely.
//
// written in: Go
// Author: Athul Muralidhar
package main
import (
    "fmt"
    "math"
)

func frange(start, end, step float64) []float64 {
    if step <= 0 || end < start {
        return []float64{}
    }
    len_arr := int((end-start)/step)
    s := make([]float64, 0,len_arr)
    for start <= end {
        s = append(s, start)
    }
}

```

```

        start += step
    }
    return s
}

func main() {
// initial Conditions
    dx := 0.1 //coordinate distance
    dt := 0.1*dx //coordinate time
    eps := 0.1
    timesteps:=int(1000/dt)
    fmt.Println(timesteps)
    x_steps := int(1000/dx)
    E_init:=0
    Eevol := make([]float64, timesteps)
    num := frange(-float64(x_steps),float64(x_steps),dx)
    TS1 := make([]float64, len(num))
    TS2 := make([]float64, len(num))
    a:= make([]float64, len(num))
    nl :=1.0
    len_TS := len(TS1)-1

// analytical oscillon solution
    a[0]=0
    TS1[0]=0
    TS2[0]=0
    for i := 1; i <len_TS; i++ {
        a[i] = 2*math.Sqrt(2.0/3.0)*(1.0/math.Cosh(float64(num[i]*eps)))

        TS1[i] = a[i]*eps
        TS2[i] = TS1[i]
    }
    TS1[len_TS]=0
    TS2[len_TS]=0

// initial energy calculation
    E_init:=0.0
    for _,val := range TS1 {
        E_init+=0.5*dx*math.Pow(val,2)
    }

//time evolution
    for t := 0; t<timesteps; t++ {
        TS3 := make([]float64, len_TS+1)
        E:=0.0
        for i := 0; i< len_TS-1; i++ {
            if i==0 {
                TS3[0]=0

```

```

        continue
    }
    phi_xx := (TS2[i+1]+TS2[i-1]-2*TS2[i])/math.Pow(dx,2)'
    phievol := (phi_xx - TS2[i]+ nl*math.Pow(TS2[i],3) -
nl*math.Pow(TS2[i],5)/math.Pow(eps,2) )*math.Pow(dt,2) + 2*TS2[i]-TS1[i]

    TS3[i]=phievol
    E+=(0.5*math.Pow((TS3[i]-TS2[i])/dt,2) + 0.5*math.Pow((TS2[i+1]-TS2[i])/dx,2
+ 0.5*math.Pow(TS2[i],2) -0.25*math.Pow(TS2[i],4))*dx
    }
    TS3[len_TS]=0
    TS1=TS2
    TS2=TS3
    E1:=E
    Eevol[t]=E1
    if t%10000==0{
        for k,val:=range TS2{
            if k==0{
                fmt.Printf("\n")
            }
            fmt.Printf("%d\t%e\n",k,val)
        }
    }
}

```

References

- [1] Mustafa A. Amin and David Shirokoff, *Flat-top oscillons in an expanding universe.*, 2010.
- [2] Evangelos I. Sfakianakis, *Analysis of Oscillons in the $SU(2)$ Gauged Higgs Model*, 2012 , arXiv:1210.7568v1
- [3] Steven C. Chapra, Raymond P. Canale, *Numerical Methods for Engineers*, Sixth Edition
- [4] William H. Press, Saul A. Teukolsky, William T. Vetterling, Brian P. Flannery, *Numerical Recipes in C*, Second Edition
- [5] R.Butt, *Introduction to Numerical Analysis using MATLAB*, 2010
- [6] Lord Rayleigh (1876). *On waves*, Philosophical Magazine, Series 5. 1 (4): 257-279
- [7] Russell Scott, 1844 *Report on Waves*, Brit. Assoc. Rep
- [8] Robert R. Long, 1964 *Solitary Waves in the Westerlies*, The Johns Hopkins University, Baltimore, Md
- [9] D.J. Korteweg and G. de Vries, *On the change of form of long waves advancing in a rectangular canal, and on a new type of long stationary waves* , Phil. Mag. (5) 39 (1895), 422–443
- [10] Clifford S. Gardner, John M. Greene, Martin D. Kruskal, and Robert M. Mira, *Method for Solving the Korteweg-deVries Equation* Phys. Rev. Lett. 19, 1095 – Published 6 November 1967
- [11] M. Remoissenet - 1999 *Waves called solitons: Concepts and experiments*, Springer. p. 11. ISBN:9783540659198.
- [12] Edwards, Harold M. (1995). *Linear Algebra*, Springer. p. 78. ISBN: 9780817637316.
- [13] R. Haberman - 2012, *Applied partial differential equations with Fourier series and boundary value problems*
- [14] Klaus Schulten, *PHYS 480 Quantum Mechanics Fall 1999*, University of Illinois at Urbana-Champaign
- [15] Karl Glasner, *Math 456: Partial differential equations*, The University of Arizona
- [16] Resnick, R.; Eisberg, R. (1985), *Quantum Physics of Atoms, Molecules, Solids, Nuclei and Particles (2nd ed.)*New York: John Wiley & Sons. ISBN: 0-471-87373-X.

- [17] C. F. Von Weizsäcker, *Probability and Quantum Mechanics*, The British Journal for the Philosophy of Science Vol. 24, No. 4 (Dec., 1973), pp. 321-337
- [18] A. O. Caldeira and A. J. Leggett, *Influence of Dissipation on Quantum Tunneling in Macroscopic Systems*, Phys. Rev. Lett. 46, 211 – Published 26 January 1981
- [19] K.A. Milton, *The Casimir effect: physical manifestations of zero-point energy*, 2001
- [20] Griffiths, David J. (2004). *Introduction to Quantum Mechanics (2nd ed.)* Prentice Hall. ISBN: 978-0-13-805326-0.
- [21] *Schrodinger equation*. hyperphysics.phy-astr.gsu.edu.
- [22] Franck, J.; Hertz, G. (1914). *On the collisions between electrons and molecules of mercury vapor and the ionization potential of the same*, Verhandlungen der Deutschen Physikalischen Gesellschaft (in German). 16: 457–467.
- [23] Gerlach, W.; Stern, O. (1922). *Der experimentelle Nachweis der Richtungsquantelung im Magnetfeld*, Zeitschrift für Physik. 9: 349–352. Bibcode:1922ZPhy.9.349G. doi:10.1007/BF01326983.
- [24] Paul G. Kwiat; H. Weinfurter; T. Herzog; A. Zeilinger; M. Kasevich (1994). *Experimental realization of interaction-free measurements*, Retrieved 2012-05-07.
- [25] Richard Feynman (1970). *The Feynman Lectures on Physics Vol II*. Addison Wesley Longman. ISBN:978-0-201-02115-8.
- [26] Daniel Baumann, *Quantum Field Theory*, Institute of Theoretical Physics, University of Amsterdam
- [27] Rajaraman, R. (1989). *Solitons and Instantons: An Introduction to Solitons and Instantons in Quantum Field Theory*, North-Holland Personal Library. 15. North-Holland. pp. 34–45. ISBN 978-0-444-87047-6.
- [28] Dodd, Roger K.; J. C. Eilbeck; J. D. Gibbon; H. C. Morris (1982). *Solitons and Nonlinear Wave Equations*, London: Academic Press. ISBN 978-0-12-219122-0.
- [29] Tsumagari, Mitsuo (2009) *The physics of Q-balls*, PhD thesis, University of Nottingham.
- [30] Maciej Dunajski, *Integrable Systems*, Department of Applied Mathematics and Theoretical Physics University of Cambridge Wilberforce Road, Cambridge CB3 0WA, UK May 10, 2012

- [31] https://www.uni-muenster.de/imperia/md/content/physik_tp/lectures/ws2016-2017/num_methods_i/sinegordon.pdf
- [32] L.D.Faddeev, V.E.Korepin, *Quantum theory of solitons*, Physics Reports Volume 42, Issue 1, June 1978, Pages 1-87
- [33] K. Nozaki, *Stochastic Instability of Sine-Gordon Solitons*, Phys. Rev. Lett. 49, 1883 – Published 27 December 1982
- [34] Costa, Giovanni; Fogli, Gianluigi (2012). *NuNSymmetries and Group Theory in Particle Physics: An Introduction to Space-Time and Internal Symmetries*, Springer Science & Business Media. p. 112
- [35] Anderson, P.W. (1972), *More is Different Science* 177 (4047): 393–396. doi:10.1126/science.177.4047.393. PMID 17796623.
- [36] Kosmann-Schwarzbach, Yvette (2010). *The Noether theorems: Invariance and conservation laws in the twentieth century. Sources and Studies in the History of Mathematics and Physical Sciences*. Springer-Verlag. ISBN 978-0-387-87867-6.
- [37] Nina Byers (1998) *E. Noether's Discovery of the Deep Connection Between Symmetries and Conservation Laws*, in Proceedings of a Symposium on the Heritage of Emmy Noether, December 1996, Bar-Ilan University, Israel, Appendix B.
- [38] http://www.damtp.cam.ac.uk/research/gr/public/cs_top.html
- [39] S. Coleman (1985). *Q-Balls*, Nuclear Physics B. 262 (2): 263. Bibcode:1985NuPhB.262..263C. doi:10.1016/0550-3213(85)90286-X.
- [40] <http://hyperphysics.phy-astr.gsu.edu/hbase/quantum/qmoper.html>
- [41] http://www.tcm.phy.cam.ac.uk/~bds10/aqp/handout_operator.pdf
- [42] Robert Weinstock, *Calculus of Variations: With Applications to Physics and Engineering*, Dover Publications, 1974
- [43] http://ersoy.univ-tln.fr/simu/soliton_et0.avi.mp4.jpg
- [44] Stefan Antusch , Francesco Cefalà , Sven Krippendorf , Francesco Muia , Stefano Orani and Fernando Quevedo , *Oscillons from String Moduli*, arXiv:1708.08922v1, Aug 2017
- [45] Lemaître, G. (1931). *A Homogeneous Universe of Constant Mass and Growing Radius Accounting for the Radial Velocity of Extragalactic Nebulae*. Monthly Notices of the Royal Astronomical Society. 91 (5): 483–490. Bibcode:1931MNRAS..91..483L. doi:10.1093/mnras/91.5.483.

- [46] Hubble, E. (1929). *A Relation Between Distance and Radial Velocity Among Extra-Galactic Nebulae*. Proceedings of the National Academy of Sciences. 15 (3): 168–73. Bibcode:1929PNAS...15..168H. doi:10.1073/pnas.15.3.168. PMC 522427 Freely accessible. PMID 16577160.
- [47] White, M. (1999). *Anisotropies in the CMB*. Proceedings of the Los Angeles Meeting, DPF 99. UCLA. arXiv:astro-ph/9903232 Freely accessible. Bibcode:1999dpf.conf.....W
- [48] Fixsen, D. J. (2009). *The Temperature of the Cosmic Microwave Background*. The Astrophysical Journal. 707 (2): 916–920. arXiv:0911.1955 Freely accessible. Bibcode:2009ApJ...707..916F. doi:10.1088/0004-637X/707/2/916.
- [49] Daniel Baumann, *Cosmology*, <http://cosmology.amsterdam/education/cosmology/>
- [50] Spergel, D.N. (2006). *Three-year Wilkinson Microwave Anisotropy Probe (WMAP) observations: Implications for cosmology*.
- [51] Mustafa A. Amin, Richard Easther, Hal Finkel, Raphael Flauger and Mark P. Hertzberg , *Oscillons After Inflation*, arXiv: 1106.3335v2
- [52] Jing Liu, Zong-Kuan Guo, Rong-Gen Cai and Gary Shiu *Gravitational Waves from Oscillons with Cuspy Potentials*, arXiv:1707.09841v2
- [53] Mustafa A. Amin, Richard Easther and Hal Finkel, *Inflaton Fragmentation and Oscillon Formation in Three Dimensions*, arXiv: 1009.2505v2
- [54] Eric Cotner, Alexander Kusenko and Volodymyr Takhistov, *Primordial Black Holes from Inflaton Fragmentation into Oscillons* arXiv:1801.03321v1
- [55] N. Graham , *Numerical Simulation of an Electroweak Oscillon*, arXiv: 0706.4125v2
- [56] Evangelos I. Sfakianakis , *Analysis of Oscillons in the $SU(2)$ Gauged Higgs Model*,
- [57] N. Graham, *An Electroweak Oscillon*, arXiv:hep-th/0610267
- [58] Marcelo Gleiser, Noah Graham and Nikitas Stamatopoulos , *Generation of Coherent Structures After Cosmic Inflation*, arXiv:1103.1911v2
- [59] E. Farhi, N. Graham, V. Khemani, R. Markov, R. Rosales, *An Oscillon in the $SU(2)$ Gauged Higgs Model*, C: arXiv:hep-th/0505273